

**Second Quarterly Report  
for  
FEASIBILITY OF GROUND-PENETRATING RADAR  
FOR USE AT MGP SITES**

Pawan Chaturvedi, Richard G. Plumb & Kenneth R. Demarest

Radar Systems and Remote Sensing Laboratory  
Department of Electrical and Computer Engineering, University of Kansas  
2291 Irving Hill Road, Lawrence, Kansas 66045-2969  
TEL: 913/864-4835 \* FAX: 913/864-7789 \* OMNET: KANSAS.U.RSL \* TELEX: 706352

RSL Technical Report 9990-2

April 1993

Sponsored by:

Electric Power Research Institute, Inc.  
P. O. Box 10412, Palo Alto CA 94303

Agreement RP 2879-27

“DISCLOSURE”

This report has not been reviewed to determine whether it contains patentable subject matter, nor has the accuracy of its information or conclusions been evaluated. Accordingly, the report is not considered a published report and is not available for general distribution, and its distribution is limited to employees and advisors of EPRI for the sole purpose of evaluating the progress and the future course of the project described in the report. Until the report has been reviewed and evaluated by EPRI, it should be neither disclosed to others nor reproduced, wholly or partially, without written consent of EPRI.

The University of Kansas, Center for Research Inc.

## Table of Content

1. Summary.....	4
2. Introduction.....	6
3. Reconstruction Algorithm.....	9
4. Simulations and Results.....	13
5. Field Implementation.....	27
6. Conclusions.....	28
7. Future Work.....	29
8. References.....	30

## 1. Summary

This is the second quarterly report for the research project, "Feasibility of Ground Penetrating Radar for Use at MGP Sites," EPRI Agreement RP2879-27. This report covers the period from January 1, 1993 through March 31, 1993.

The goal of this investigation is to identify and implement a technique for imaging subsurface spill sites. In the first quarter of the project, the technique to be used for this investigation was identified as diffraction tomography. This technique can be used to obtain high quality images of objects buried in optically opaque media by measuring the scattered fields from the object [1],[2]. Since in principal, the transmitters and the receivers can be placed anywhere in space, it is possible to place all the transmitters and the receivers on the surface. But one of the assumptions in the development of this technique is that the object is weakly scattering, implying that most of the scattered field lies in the forward direction. Furthermore, the fields suffer attenuation while propagating through ground, and the propagation characteristics of the fields depend strongly on the soil properties at the site. Due to these reasons, the surface-to-surface geometry may not result in the detection of the object. Hence, it is proposed that a preliminary survey of the site be done with a ground penetrating radar or a surface-to-surface arrangement to determine if a more accurate survey is needed. Then, offset VSP tomography may be needed to obtain images of better quality and higher resolution.

During the past three months, the theoretical results presented in the first quarterly report were implemented on a computer. Diffraction tomography is being used as the technique to do the post-processing after the data has been collected using a Ground Penetrating Radar. In the first report, the theory behind this technique was described in detail. A reconstruction algorithm was presented, and various techniques for the reconstruction of the image of the subsurface object were mentioned. In the second phase of the project, the models developed earlier were implemented on the computer. The reconstruction algorithm used for this work is the filtered backpropagation algorithm instead of the direct Fourier inversion technique as was mentioned in the first report.

Simulation studies were done for the phase of the project using a simple test object. The image of the test object was reconstructed using this technique for different sets of parameters for the test object. Only two-dimensional objects have been considered in this work, but the results can be extended to three dimensional geometries after some modifications. The scattered field data were generated using the analytic expressions available for the objects considered in this report. It was assumed that the object is buried in a lossless, homogeneous background. The results for the simulations are presented in this report. This technique results in fairly good reconstruction of the

objects considered. The various limitations and the direction of the future work are mentioned towards the end of this report.

In the next phase of the project, it is proposed that the Finite-Difference Time-Domain (FDTD) technique be used to model more complex geometries than those considered so far, so that a larger class of objects can be investigated. Since the biggest limitation of this technique is the assumption of weak scattering by the object being imaged, the use of more robust reconstruction schemes like the iterative Born approximation instead of a first-order Born approximation or the Rytov approximation will be investigated. The results for different geometries of the transmitter and receiver locations, and the improvement achieved in the image quality by varying the operating frequency also need to be investigated.

## 2. Introduction

In the first phase of this project, the feasibility of using diffraction tomography for detection and imaging of subsurface spill sites was investigated. This was documented in the first quarterly report submitted for this project. An extensive literature survey was done to evaluate the various techniques available and to investigate the advantages and limitations of diffraction tomography technique for such applications.

From the literature survey, it was concluded that the diffraction tomography technique provides a useful and accurate technique for imaging of objects buried in an optically opaque medium. It has been used extensively in medical imaging for several years. But its application to geophysics and non-destructive testing has not been as widespread, and its potential for such applications has only recently been acknowledged.

Diffraction tomography provides a good resolution imaging technique for subsurface imaging and other geophysical applications. The image of an underground formation or object is reconstructed from the scattered field data collected at the site. The Fourier transform of the scattered field is related to the object profile that caused the scattering taken along semicircular arcs. The orientation of the arc depends on the line of observation, and its location in the  $k$ -space depends on the angle of the incident plane wave. By measuring the scattered field, and using the relationship between the Fourier transforms of the object profile and the scattered field, the image can be reconstructed. In principle, the process of reconstruction reduces to estimating the object profile from its values at a finite number of discrete points in space at which its Fourier transform is available from the scattered fields.

Various techniques have been employed in the past to obtain the object profile from its Fourier transforms at discrete points in  $k$ -space. Two of the most popular techniques are the direct interpolation method and the filtered backpropagation algorithm. In the interpolation technique, the Fourier transform of the object profile is obtained on a rectangular grid from its values at known points by an interpolation scheme, and an inverse transform of these values directly gives the object profile. In the reconstruction process based on the filtered backpropagation algorithm, the object profile is obtained without any interpolation by using a spatial filter at each point. Since the scattered field is related to the Fourier transform of the object profile along semicircular arcs, the process of image reconstruction is a non-trivial problem.

In geophysical problems, the reconstruction process becomes even more complicated due to the unavailability of view angles all around the object, unlike in medical imaging. Furthermore,

a lossy background and the need for good resolution present two seemingly contradictory requirements on the operating frequency. Whereas the losses are lower at lower frequencies, the resolution degrades at lower frequencies. Since the best possible k-space coverage for diffraction tomography is limited to a disc of radius  $\sqrt{2}k$ , where  $k$  is the wavenumber in the background medium, using a lower frequency also results in a smaller coverage of the object in k-space, degrading the quality of the image further.

Thus, an appropriate choice of the geometry of the transmitter and receiver locations and the operating frequency is critical to the quality of the image. Offset VSP (vertical seismic profiling) provides a convenient geometrical setup of the transmitters and receivers with a reasonable k-space coverage. For this reason, it was chosen as the geometrical arrangement used for this project. For simulations, frequencies of 100 MHz and 200 MHz are currently being used, and the effect of changing frequencies on the reconstruction is being investigated. It is anticipated that the operating frequency would not exceed these values because of the high attenuation suffered at higher frequencies while propagating in the ground.

Another key requirement for the success of this technique is the validity of the weak scattering approximation, as was mentioned in the earlier report. Since the reconstruction algorithms assume a weakly scattering object for simplification, this imposes a limitation on the quality of the image. This poses possibly the biggest limitation on this technique. This issue is being examined carefully, and some of the results are presented in this report. Two common weak scattering approximations employed in electromagnetics are the Born and the Rytov approximations. Although both assume the object to be weakly scattering, the conditions required for the validity of the two approximations are different.

Whereas the Born approximation puts a limitation on the object profile as well as the spatial extent of the scatterer, Rytov approximation does not require any limitation on size of the object. On the other hand, the Rytov approximation is more sensitive to the changes in the object profile. So the Rytov approximation breaks down more gracefully as the size of the object is increased, compared to the Born approximation. For larger contrasts between the permittivity of the object and the background medium, Born approximation is probably more appropriate if the size of the object is small. The Born approximation is also simpler to implement. Thus, neither one of these approximations can be considered to be universally more advantageous than the other. Results for various sizes and contrasts of the object are presented later in this report.

In the progress report submitted earlier for the first phase of the project, the theoretical aspects of the technique were discussed and an outline for the application of the technique to

geophysical applications was presented. The issues of parameter selection and reconstruction were discussed and a reconstruction algorithm was proposed. It was proposed that the direct interpolation-based algorithm would be used for reconstruction since it eliminates the need for applying the spatial filter required for each point for the filtered backpropagation algorithm. During the investigation of the various options, it was found that the filtered backpropagation algorithm is conceptually a much simpler algorithm for implementation. In most cases, the interpolation process itself requires substantial computation, neutralizing somewhat the savings in computational time obtained by avoiding the spatial filtering process. So the filtered backpropagation algorithm is being used for reconstruction in the simulations for this part of the project. The issue of saving in computational time is also being investigated to make the reconstruction process optimal in terms of computational time. The reconstruction process being used is based on the filtered backpropagation algorithm proposed by Devaney [3], [4], and will briefly be described in the next section.

This report summarizes the work done since the writing of the first report. The emphasis in this report is on the description of the simulations done for testing this technique and the implementation of the algorithm based on the theoretical considerations discussed in the first report. Some results have been obtained for simple simulated test objects, and they are included in this report.



### 3. Reconstruction Algorithm

There are two popular reconstruction algorithms used for the reconstruction of the image in diffraction tomography, namely, the direct interpolation and the filtered backpropagation algorithms. In the direct interpolation algorithm, the Fourier transform of the object profile is obtained at points on a rectangular grid as mentioned earlier [5],[6]. This is accomplished by using an interpolation scheme to evaluate the object profile at discrete points on a rectangular grid from the values obtained from the scattered field data. The object profile is available on a set of points on semicircular arcs. Thus, the interpolation has to be done for points on a rectangular grid from the values available on a circular grid. Once the Fourier transform has been obtained on a rectangular grid, the object profile can be obtained by a direct Fourier inversion.

The other well-known technique used for image reconstruction is the filtered backpropagation algorithm [3],[4]. This algorithm does not require the interpolation of the object profile from a circular grid onto a rectangular grid, as required for a direct Fourier inversion. This is a non-linear transformation. In the filtered backpropagation algorithm, the measured fields are propagated backwards into the object from the receivers. A spatial filter is used to reconstruct the image of the object. The details of this reconstruction algorithm have been described by Devaney [3],[4]. Here, a brief overview of the algorithm is presented for completeness.

Consider a subsurface object surrounded by a homogeneous background as shown in Fig. 1. Assume a plane wave illumination of the object, which can be achieved from the line sources by using a technique similar to the plane wave stacking used in geophysics [3],[7]. The figure shows the geometry for an offset VSP arrangement. All the transmitters are placed on the surface, whereas the receivers are placed in a vertical borehole.  $\phi_0$  is the angle of incidence that the incident plane wavevector  $\mathbf{s}_0$  makes with the positive x-axis. For the offset VSP, the maximum angular coverage achievable is  $\phi_0 = 0$  to  $\phi_0 = -\pi$ . The practical considerations will further limit the angular coverage. Throughout this report, only two-dimensional objects will be considered for simplicity. The same concepts can be extended to the three-dimensional case with a few modifications. Define the object profile as

$$O(\mathbf{r}) = 1 - \frac{C_0^2}{C^2(\mathbf{r})} \quad (1)$$

where  $C_0$  is the velocity of the wave in the embedding medium and  $C(\mathbf{r})$  is the velocity in the object profile. In general,  $C(\mathbf{r})$  is complex, so the reconstruction of the object profile gives both the phase velocity and the attenuation profile of the object. For an incident plane wave described by

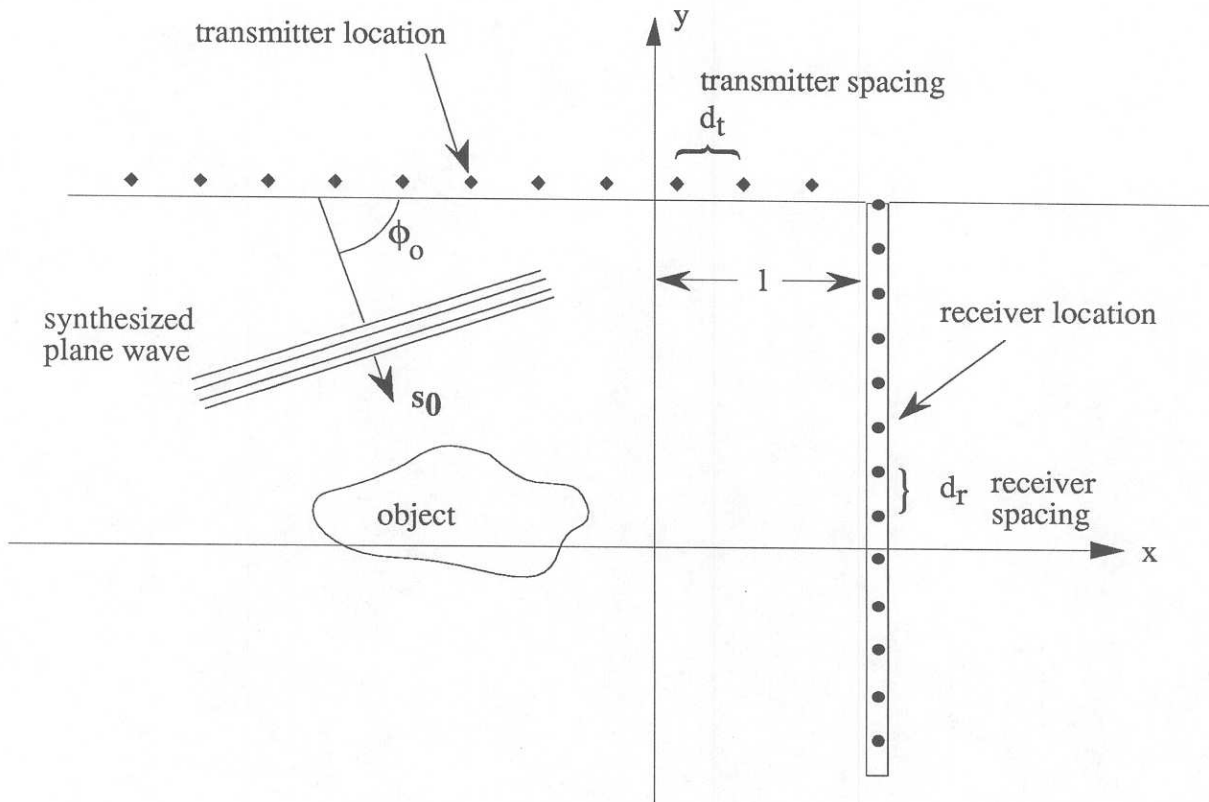


Fig. 1. Diffraction tomography with offset VSP

$$U(\mathbf{r}) = U_0 \exp(j\mathbf{k} \cdot \mathbf{s}_0 \cdot \mathbf{r}) \quad (2)$$

the two-dimensional Fourier transform of this object profile is related to the one-dimensional Fourier transform of the scattered field by

$$O(\mathbf{k}(\mathbf{s}-\mathbf{s}_0)) = \begin{cases} \frac{j 2 \gamma \exp(-j \gamma l)}{k_0^2 U_0} U_s(\kappa) & \text{for Born Approximation} \\ \frac{j 2 \gamma \exp[-j(\gamma - \kappa s_{0x})l]}{k^2 U_0} \psi(\kappa - \kappa s_{0y}) & \text{for Rytov Approximation} \end{cases} \quad (3)$$

where  $U_s$  denotes the scattered field and

$$\mathbf{s} = \frac{1}{k} (\gamma \mathbf{x} + \kappa \mathbf{y}) \quad (4)$$

with  $\gamma = \sqrt{k^2 - \kappa^2}$ . The complex phase for the Rytov approximation is defined by the equation,

$$U(\mathbf{r}, \mathbf{s}_0) = U_0 \exp(\Psi(\mathbf{r}, \mathbf{s}_0)) \quad (5)$$

The notation here has been modified from that used in the first quarterly report to make minimal changes in the description of the reconstruction algorithm given by Devaney [3]. This relationship between the Fourier transform of the object profile and the Fourier transform of the scattered field

can be used to reconstruct the image of the object from the scattered field measurements. The results for the Born and the Rytov approximations can be conveniently combined by defining the "data"  $D(y, \mathbf{s}_0)$  as

$$D(y, \mathbf{s}_0) = \begin{cases} \frac{j}{k_0^2} \frac{2}{U_0} U_s(y) & \text{for Born Approximation} \\ \frac{j}{k^2} [\Psi(\mathbf{r}_0, \mathbf{s}_0) - j\mathbf{k} \cdot \mathbf{s}_0 \mathbf{r}_0] \exp(j\mathbf{k} \cdot \mathbf{s}_0 \mathbf{r}_0) & \text{for Rytov Approximation} \end{cases} \quad (6)$$

The relationship in Eq. (3) can now be written as

$$D(\kappa, \mathbf{s}_0) = \frac{e^{j\gamma l}}{\gamma} \tilde{O}(\gamma - \kappa s_{0x}, \kappa - \kappa s_{0y}) \quad (7)$$

where  $\tilde{O}$  represents the two-dimensional Fourier transform of the object profile,

$$\tilde{O} = \int d^2\mathbf{r} O(\mathbf{r}) e^{-j\mathbf{K} \cdot \mathbf{r}} \quad (8)$$

where  $\mathbf{K} = (\gamma - \kappa s_{0x}) \mathbf{x} + (\kappa - \kappa s_{0y}) \mathbf{y}$  defines semicircular arcs of radius  $k$  in  $k$ -space, with centers at  $\mathbf{K} = -\kappa \mathbf{s}_0$ .

The backpropagation algorithm for the reconstruction of the object profile uses the fact that the maximum  $k$ -space coverage for diffraction tomography is limited to a disc of radius  $\sqrt{2}k$  in the  $k$ -space. So the image obtained by this technique is a low-pass version of the actual object. The object profile is reconstructed by using an appropriate low-pass filter. An inversion formula based on the spatial filtering operation has been obtained by Devaney [4]. For two-dimensional objects, the reconstructed object profile can be evaluated from

$$O(\mathbf{r}) = \frac{k^2}{2(2\pi)^2} \int_{S_0} d\phi_0 \int_S d\phi \sqrt{1 - (\mathbf{s} \cdot \mathbf{s}_0)^2} \gamma D(\kappa, \mathbf{s}_0) e^{-j\gamma l} e^{j[(\gamma - \kappa s_{0x})x + (\kappa - \kappa s_{0y})y]} \quad (9)$$

where  $S_0$  is the set of all the available values of  $\phi_0$ . Thus the object profile is reconstructed from the data by first computing the partial reconstructions for every angle of incidence  $\phi_0$  and then combining all the partial reconstructions to obtain the object profile. For the geophysical applications, this filter can be broken down into a stationary convolutional filter  $F(\kappa, \phi_0) \Theta(\kappa, \phi_0)$  and a space varying filter  $e^{j[\gamma(x-l) + \kappa y]}$  such that each partial reconstruction is obtained as

$$O_0(\mathbf{r}, \mathbf{s}_0) = \frac{k}{2\pi} e^{-j\kappa \mathbf{s}_0 \cdot \mathbf{r}} \int_{-\infty}^{\infty} d\kappa F(\kappa, \phi_0) \Theta(\kappa, \phi_0) D(\kappa, \mathbf{s}_0) e^{j[\gamma(x-l) + \kappa y]} \quad (10)$$

where  $F(\kappa, \phi_0) = 0$  for  $|\kappa| \geq k$ , and for  $|\kappa| \leq k$ ,

$$F(\kappa, \phi_0) = \begin{cases} 0 & \text{if } \kappa \geq -k \sin \phi_0 \text{ with } -\pi \leq \phi_0 \leq -\pi/2 \\ |\kappa \cos \phi_0 - \gamma \sin \phi_0| & \text{otherwise} \end{cases} \quad (11)$$

$\Theta(\kappa, \phi_0) = 1$  for a complex profile, and

$$\Theta(\kappa, \phi_0) = \begin{cases} 0 & \text{if } \kappa \leq k \sin \phi_0 \text{ with } -\pi/2 \leq \phi_0 \leq 0 \\ 1 & \text{otherwise} \end{cases} \quad (12)$$

for offset VSP with real profile. The object profile is obtained from the partial reconstructions by combining them using

$$O(\mathbf{r}) = \frac{1}{2\pi} \int_{S_0} d\phi_0 O_0(\mathbf{r}, \mathbf{s}_0) \quad (13)$$

for complex profiles, and

$$O(\mathbf{r}) = \frac{1}{\pi} \operatorname{Re} \left\{ \int_{S_0} d\phi_0 O_0(\mathbf{r}, \mathbf{s}_0) \right\} \quad (14)$$

The reader is referred to [3] for a detailed description and the derivation of the spatial filters. Using this reconstruction procedure, the interpolation and Fourier inversion steps required in the direct interpolation algorithms are eliminated. For the simulations done for this project, the backpropagation algorithm has been used. In the next section, some of the results obtained with the backpropagation algorithm are presented.

## 4. Simulations and Results

A brief summary of the backpropagation algorithm was presented in the previous section of the report. Using this algorithm, simulations were done for a simple two-dimensional test object. A solid dielectric cylinder of infinite length in the z-direction was used for simulations since analytic expressions for the scattered fields from a cylinder are available. These analytic expressions for the scattered fields were coded to obtain the scattered field data. Matlab software is being used for all the simulations since many of the signal processing tools required for this work are available in Matlab, and it provides a convenient software for computations involving matrices.

Because of the weak scattering approximations used in the analysis, both the Born and the Rytov approximations are strictly valid only when the object is not a strong scatterer. But the basic requirements for the two cases are slightly different. The Born approximation requires the object to be physically small so that the total phase change over the dimensions of the object is not large. Mathematically, the requirement for the validity of the Born approximation can be stated as [8]

$$k(n-1)d \ll 1 \quad (15)$$

where  $d$  represents the size of the object and  $n$  is the deviation of the refractive index of the inhomogeneity from that of the background medium. The Rytov approximation does not require any limitation on the physical dimensions of the object. The requirement for the Rytov approximation to be valid is

$$n \gg \left[ \frac{\nabla \phi_s}{k} \right]^2 \quad (16)$$

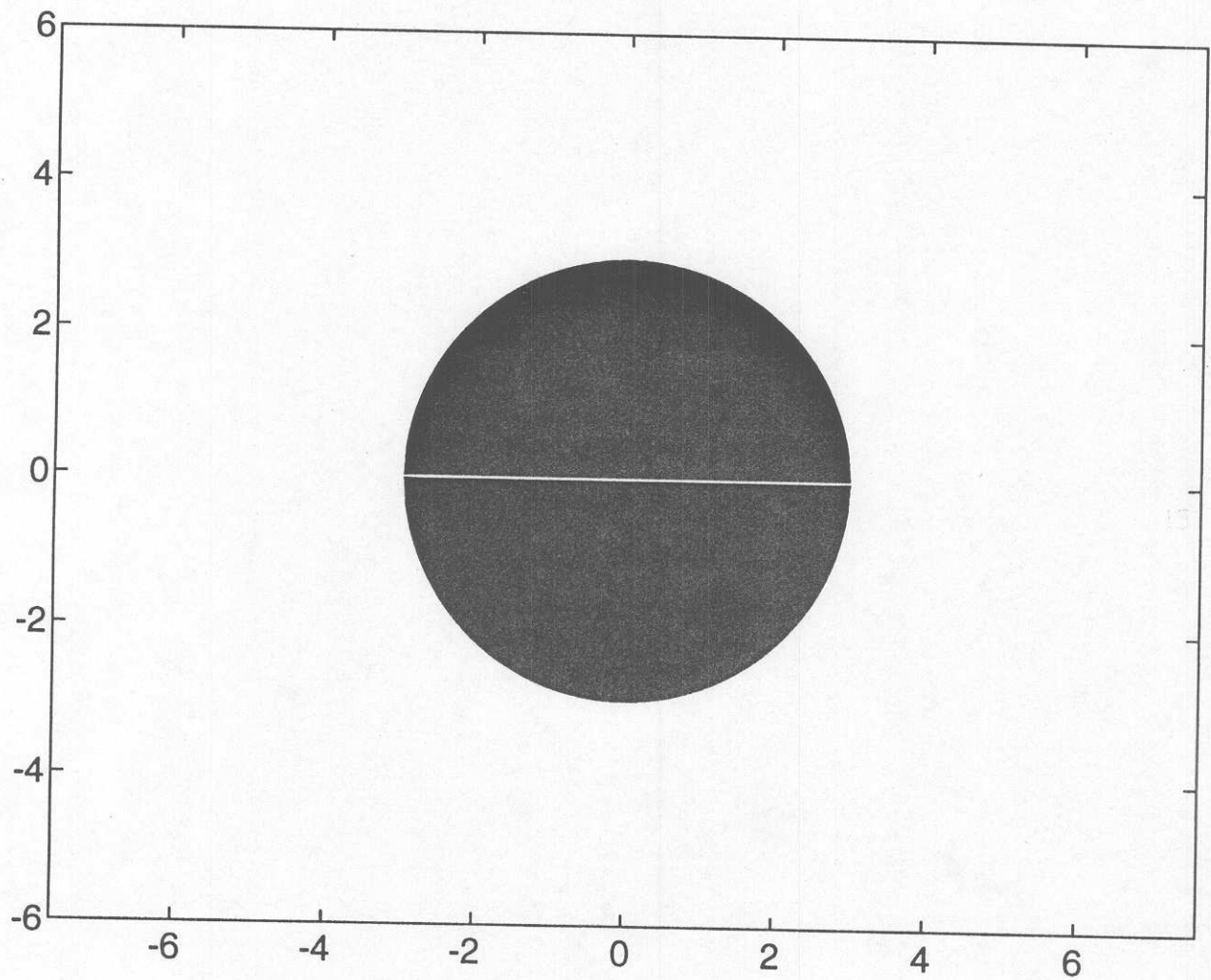
where  $\phi_s$  is the scattered phase.  $\nabla \phi_s$  represents the change in the complex scattered phase per unit distance. Thus, unlike the Born approximation, it is the change in the scattered phase over a wavelength that is important, not the total phase. The Rytov approximation is valid when the phase change over a wavelength is small.

Since the two weak scattering approximations are valid under two different set of conditions, their behavior for different properties of the scatterer are also different. The Born approximation yields better results for larger contrasts between the background permittivity and the inhomogeneity if the size of the object is kept small. But it deteriorates rapidly as the size of the object is increased. The validity of the Rytov approximation does not depend on the physical dimensions of the object. Therefore it gives much better results for larger objects, but is more sensitive to the changes in the permittivity than the Born approximation.

The test object for the simulations performed for this work was an infinitely long cylinder of radius "a." This reduces the problem to a two-dimensional problem. A plane wave illumination was assumed, and the scattered fields were computed for illumination by a plane wave. In practice, line sources would have to be used in place of plane wave sources. The plane wave response can be generated from the line sources by a procedure similar to plane wave stacking. The object was placed at the origin of the coordinate system. For all the simulations, the background permittivity is assumed to be unity and the medium is assumed to be homogeneous and lossless. Offset VSP configuration is used for the simulations. Maximum possible k-space coverage for the geometry is assumed in the reconstruction of the object profile.

The technique was tested for different values of the object profile and different sizes of the object. The test object and the results for different values of the object profile and cylinder radii are shown in figs. 2-6. The background is homogeneous in all cases, and the contrast between the object and the background is indicated in each case. As expected, the results obtained with the Born approximation are better for smaller objects, but deteriorate rapidly as the radius of the cylinder is increased. The reconstructions obtained with the Born approximation are fairly good even when the permittivity of the object compared with the background is made large, as long as the radius of the cylinder is small. On the other hand, the reconstructions achieved with the Rytov approximation are better for larger objects. But for Rytov approximation, the quality of the reconstruction is very sensitive to the permittivity contrast between the object and the background, and the quality of the images degrades rapidly as the contrast between the object and the background is increased.

Simulations were also done for a perfectly conducting cylinder to test the performance of this technique for conducting objects. Simulations were performed for both the Born and the Rytov approximations. The reconstructions are presented in fig. 7 for a conducting cylinder. It is observed that images of good quality are achieved even for a conducting object. This is because when only a single strong scatterer is present, the technique still works well since there is no multiple scattering. The performance of this technique in the presence of multiple strong scatterers has not yet been tested. The reconstruction obtained degrades. This is due to the fact that the Born approximation works best for small objects, whereas the Rytov approximation is extremely sensitive to the difference in the permittivities of the object and the background. Hence, neither the Born nor Rytov approximation provides a good reconstruction for large conducting objects.



(a)

Fig.2. The test objects used for simulations. For (a)  $ka = 2.0$ , where  $a$  is the radius of the cylinder, and  $k$  is the wavenumber. For (b),  $ka = 4\pi$ .

Fig. 2. The test objects used for simulations. For (a)  $ka = 2.0$ , where  $a$  is the radius of the cylinder, and  $k$  is the wavenumber. For (b)  $ka = 4\pi$ .

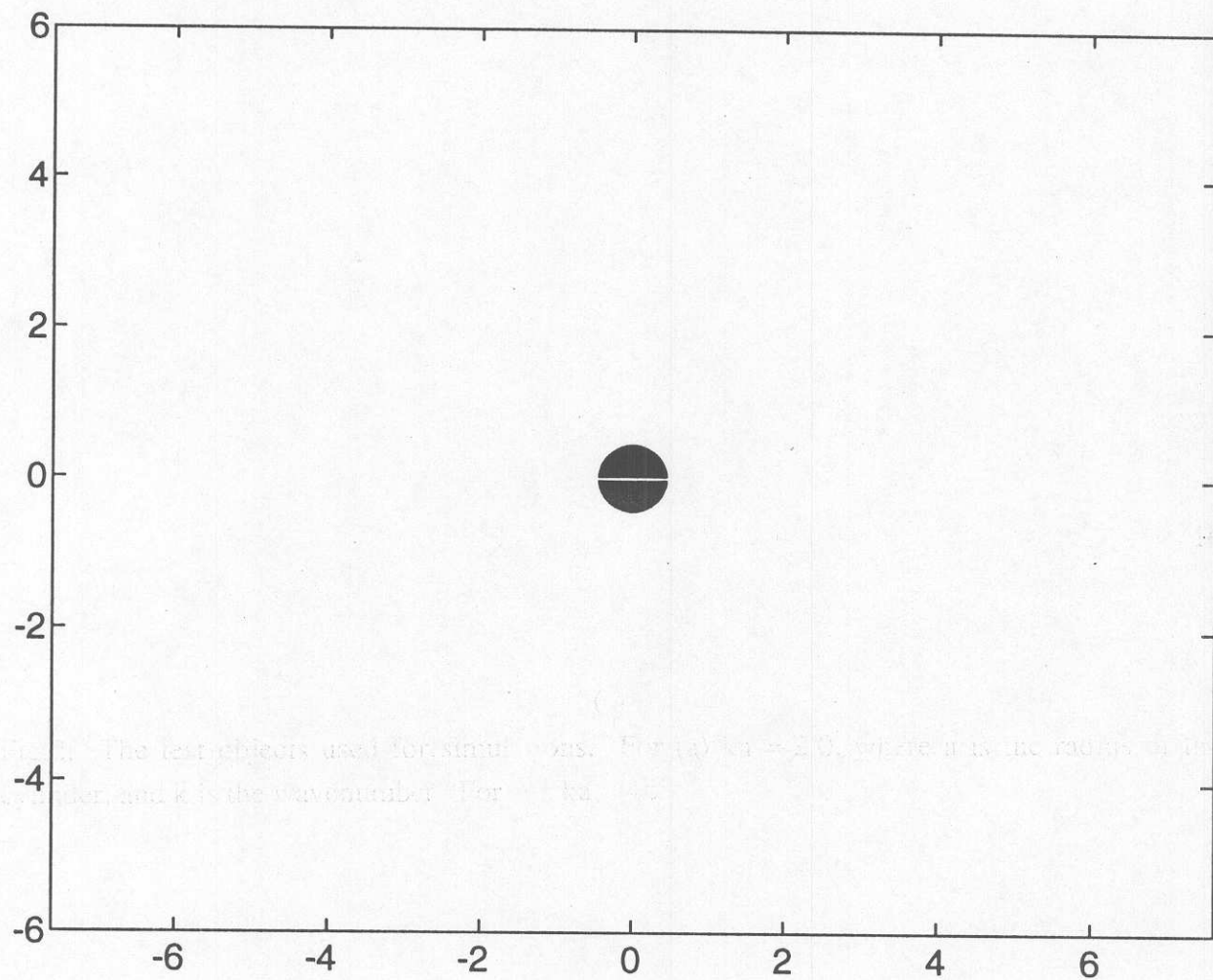
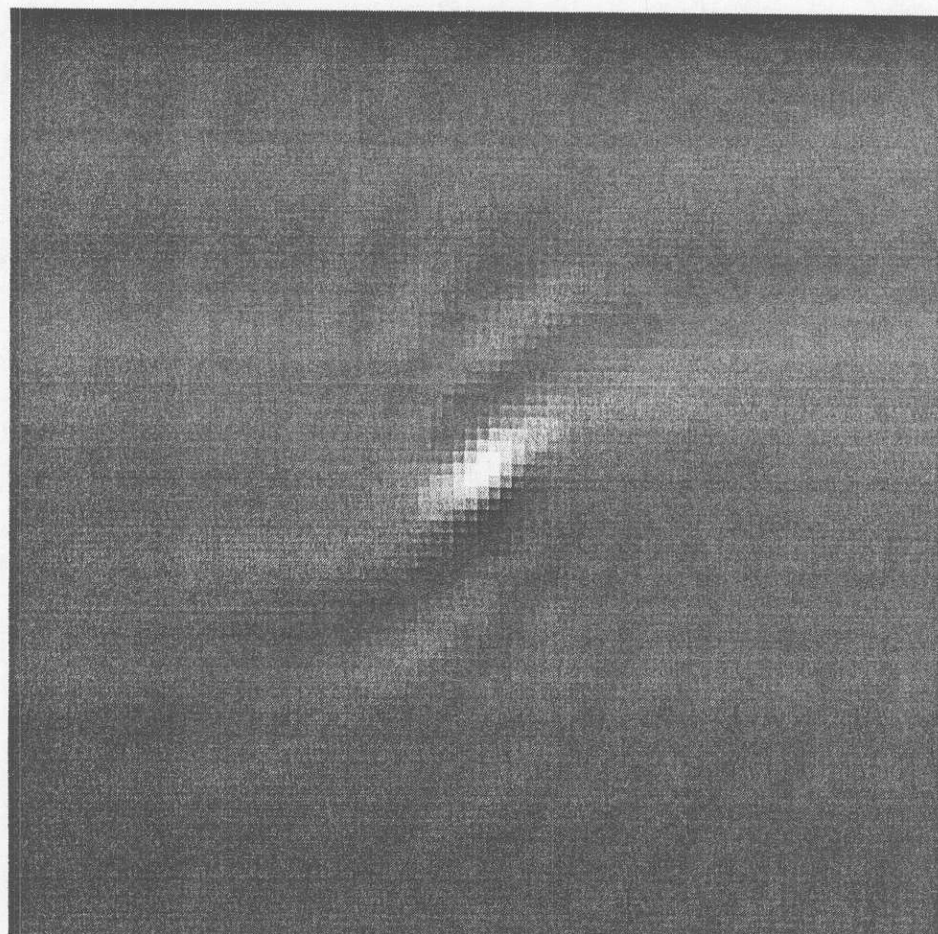


Fig.2 (b)





(a)

Fig.3. The reconstructions for (a) Born, and (b) Rytov approximations for the test object of fig. 2(a) with  $\epsilon_r = 1.01$  for the object.

The reconstructions for (a) Born, and (b) Rytov approximations for the test object of Fig. 2(a) with  $\epsilon_1 = 1.01$  for the object.

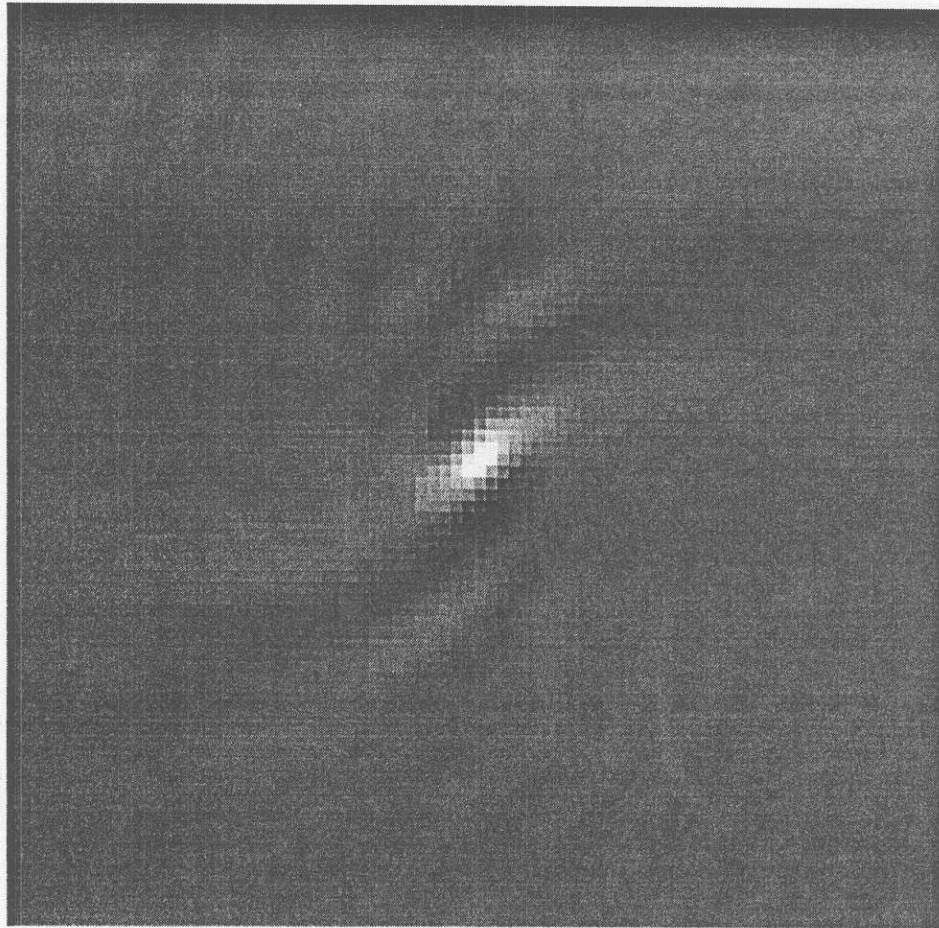
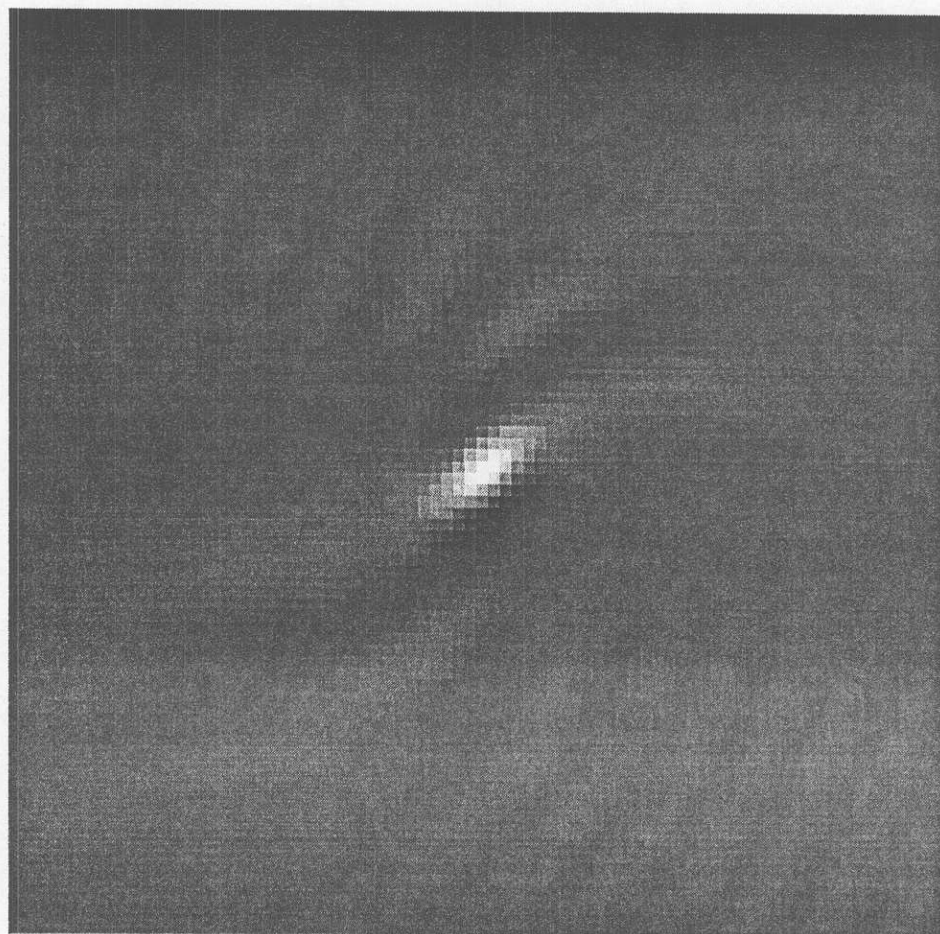


Fig.3 (b)

Fig. 4(a)



19

(a)

Fig.4. The reconstructions for (a) Born, and (b) Rytov approximations for the test object of fig. 2(a) with  $\epsilon_r = 1.20$  for the object.

19

Fig.4 The reconstructions for (a) Born, and (b) Rytov approximations for the test object of Fig. 2(a) with  $\epsilon_r = 1.20$  for the object.

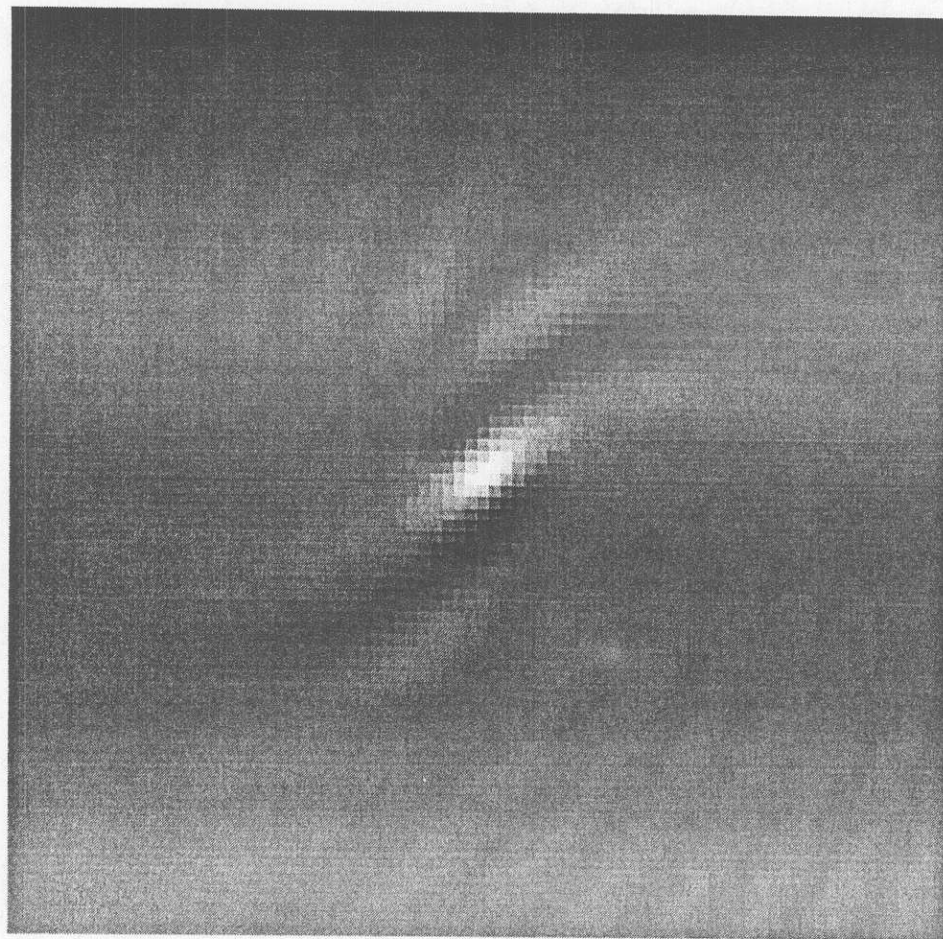
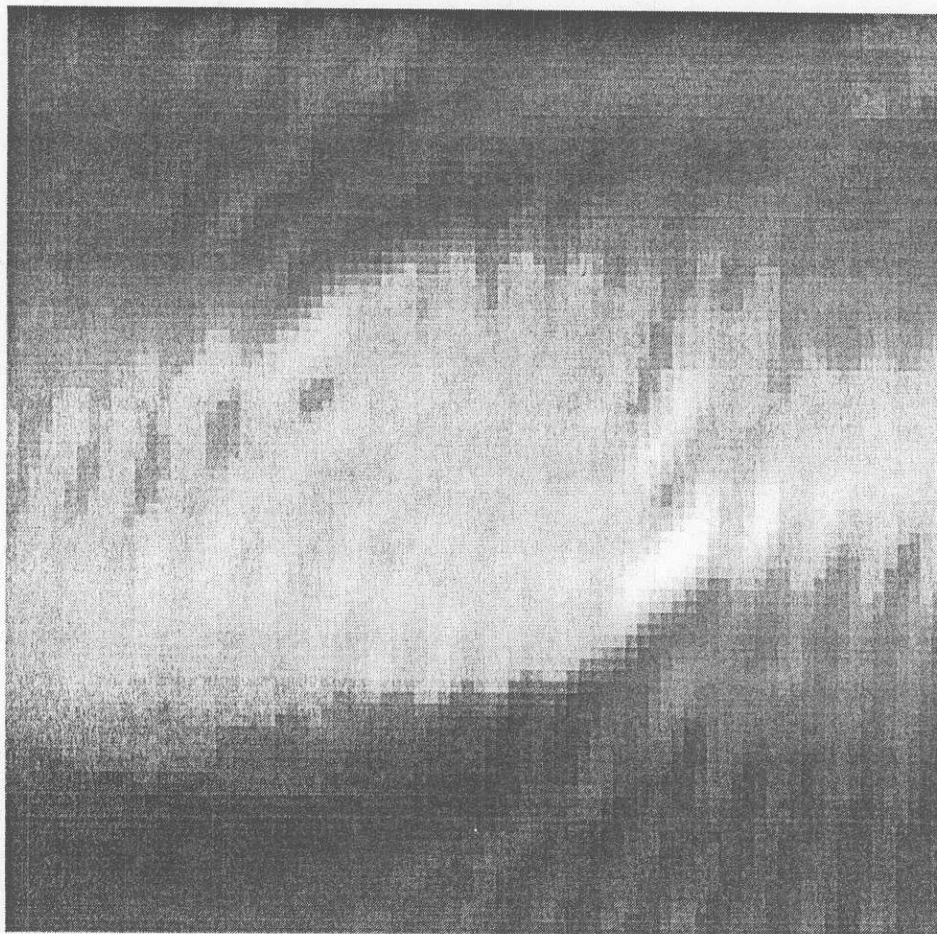


Fig.4 (b)



(a)

Fig.5. The reconstructions for (a) Born, and (b) Rytov approximations for the test object of fig. 2(b) with  $\epsilon_r = 1.01$  for the object.

Fig.5. The reconstructions for (a) Born and (b) Rytov approximations for the test object of Fig. 2(b), with  $\epsilon = 1.01$  for the object.

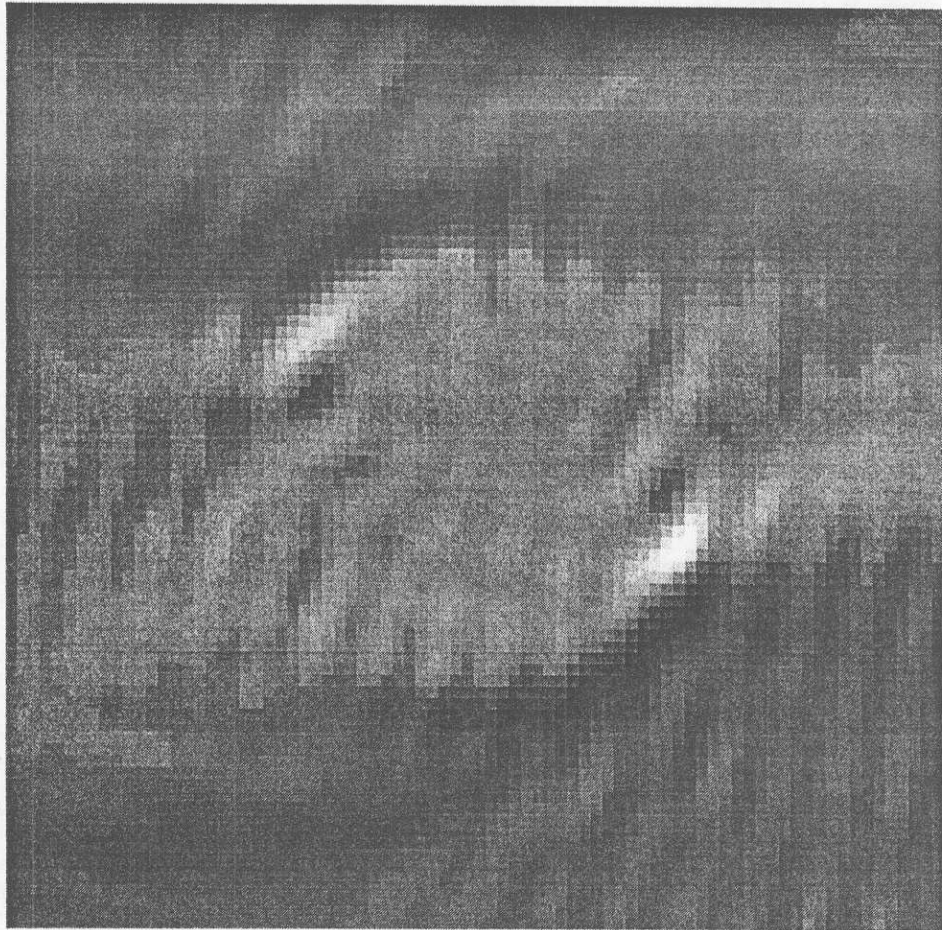
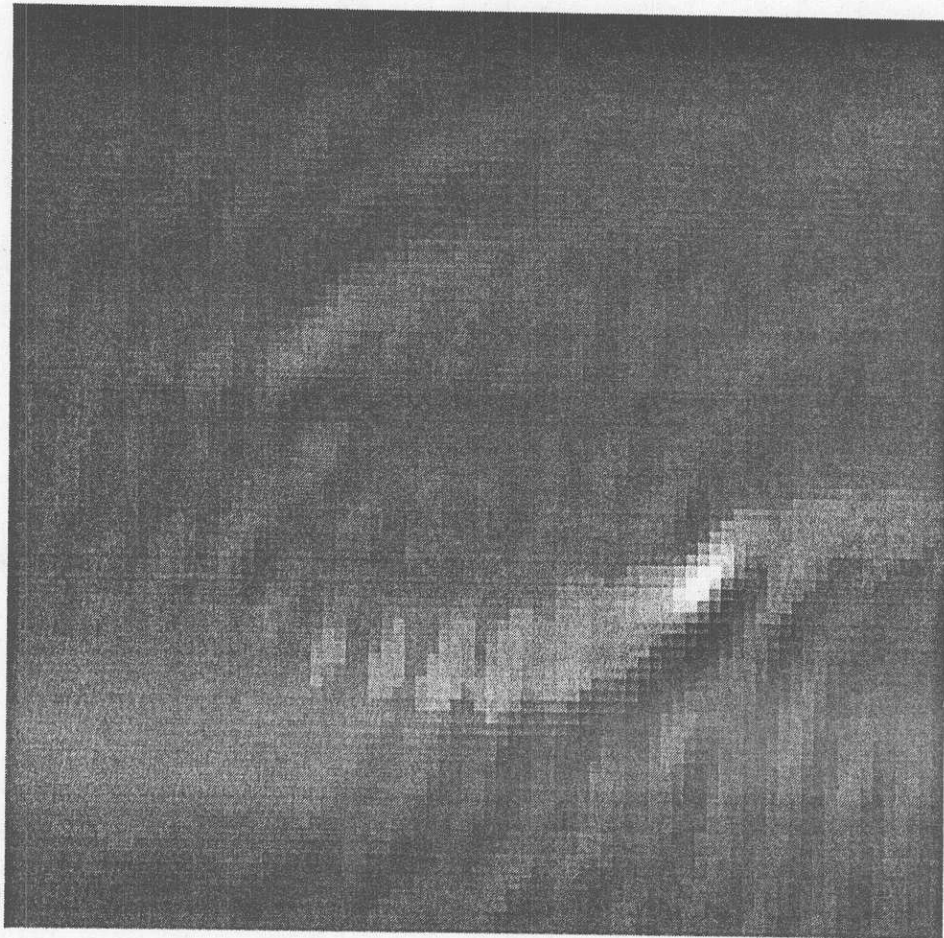


Fig.5 (b)

Fig. 6



(a)

Fig. 6. The reconstructions for (a) Born, and (b) Rytov approximations for the test object of fig. 2(b) with  $\epsilon_r = 1.20$  for the object.

FIG.6. The reconstructions for (a) Potts and (d) Rvayov approximations for the test object with  $\sigma = 1.0$  for the object.

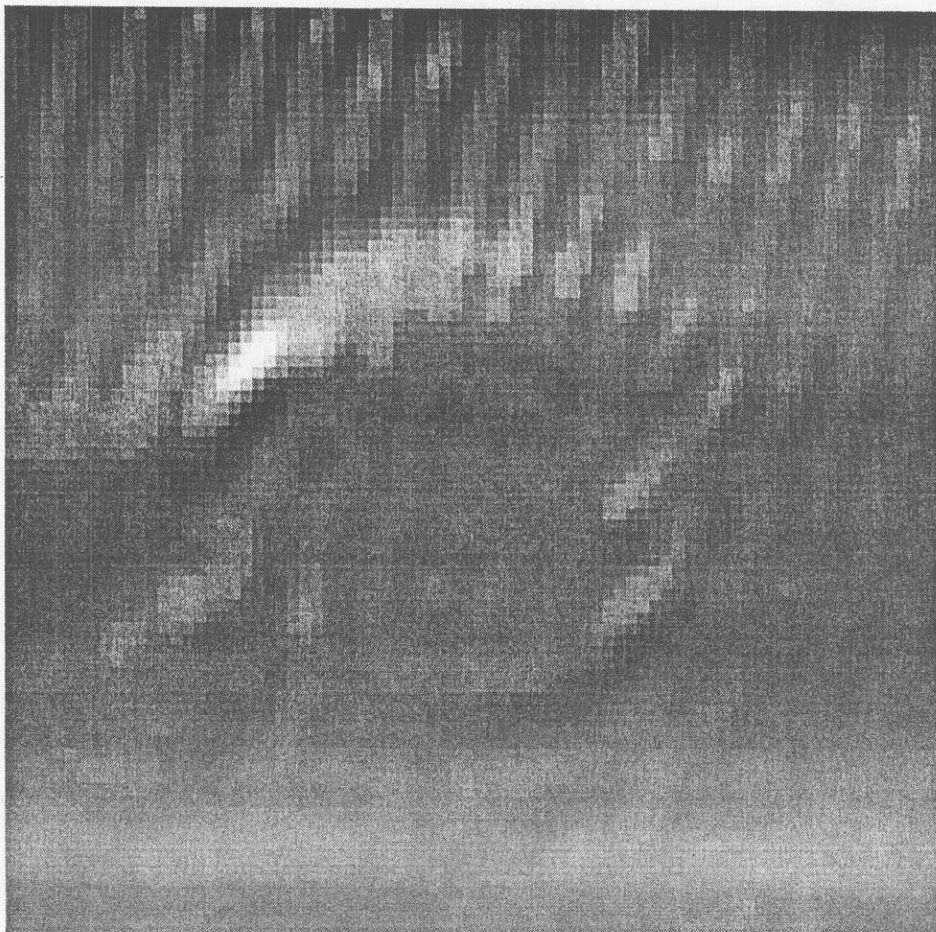
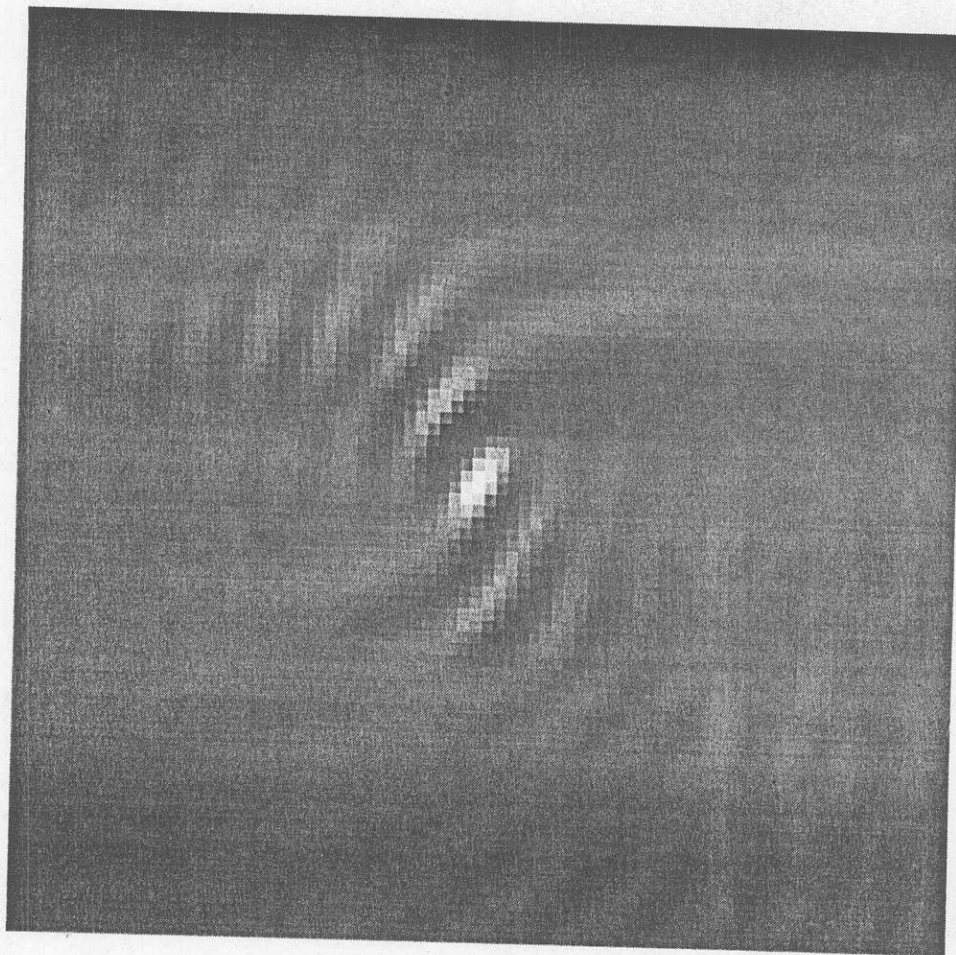


Fig.6 (b)





(a)

Fig.7. The reconstructions for (a) Born, and (b) Rytov approximations for the test object of fig. 2(a) with a perfectly conducting cylinder.

Fig.7. The reconstructions for (a) BOLA and (b) Rylov approximations for the test object (a) in fig. 2(a) with a perfectly coaxial cylinder

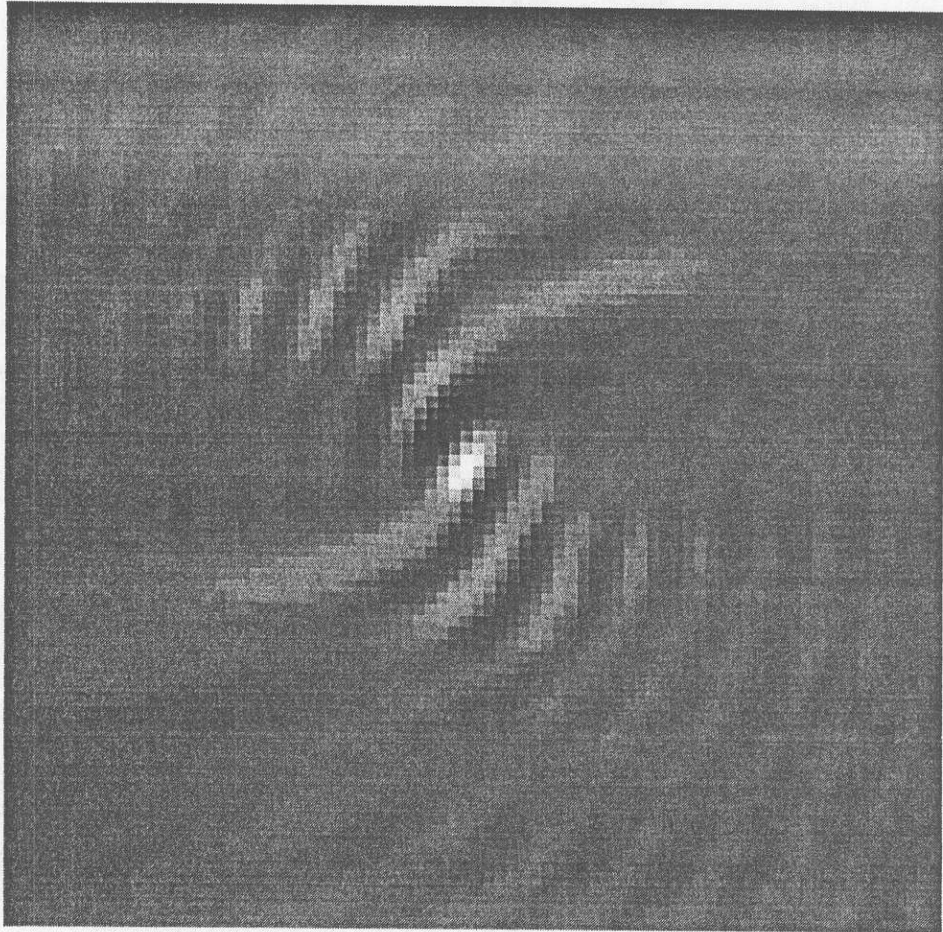


Fig.7 (b)

## 5. Field Implementation

The simulations being performed are to test the feasibility of implementing this technique on the field. The results obtained from the simulations indicate that subsurface spills can be imaged by this technique with good resolution. It is proposed that the field implementation of this technique would require two basic steps.

In the first step, a surface-to-surface survey would be done as a preliminary step to check for a spill. This would be performed by using a ground penetrating radar located on the surface. Since the basic technique used is the same as that being used for offset VSP in the simulations, the code that has been developed already can handle this geometry with some modifications. This is being done to perform the simulations for surface-to-surface tomography. This geometry would give a lower resolution image of the subsurface object because of the lower k-space coverage and the assumption that the object is weakly scattering, which implies that most of the scattered field lies in the forward direction.

Once a preliminary survey has been done, it would be known if there is a spill. Then a borehole can be drilled in the ground to perform the offset VSP tomography. The offset VSP technique would give a higher quality image and greater resolution since the k-space coverage for this case is better than the surface-to-surface geometry, and, by using offset VSP, forward scattered fields are also measured. If it is determined from the preliminary survey that there is no spill on the site, offset VSP tomography is not needed. Thus, a preliminary survey would be helpful in determining the need for a more complicated and accurate investigation.

## 6. Conclusions

The application of the diffraction tomography technique to geophysical applications like subsurface imaging has been limited. But it holds immense potential for such applications despite its limitations, and its applications in geophysical applications have developed rapidly over the past few years.

In this phase of the project, simulations were performed to image subsurface objects of simple shapes. The reconstruction was performed using the backpropagation algorithm. Simulations were done for a simple test object for which "perfect" data could be generated on the computer using the analytic expressions available. The performance of this technique under different sets of conditions was investigated. It was observed that this technique provides images of fairly good quality for many classes of objects.

The Born approximation provides better images with smaller objects and higher permittivity contrasts, whereas the Rytov approximation provides better images for smaller contrasts, but its performance does not deteriorate as the size of the object is increased. Thus, it can be concluded that neither technique is universally superior to the other, and both have relative merits and drawbacks. At sufficiently low frequencies, the Born approximation may be more attractive compared to the Rytov approximation because of its simplicity and the validity of small object size for a larger class of objects. The Born approximation also appears to work better for larger difference between the permittivity of the object and the background medium.

Good quality object reconstructions can be obtained with diffraction tomography even for conducting objects and single strong scatterers. This fact appears to be promising for the field implementation of this technique. The performance of this technique in the presence of multiple strong scatterers has not been investigated yet.

## 7. Future Work

The effect of limiting the angular coverage compared to the full offset VSP coverage, and the use of different geometries like the cross-borehole and the surface-to-surface arrangements, is being investigated. Further investigation needs to be done to determine the performance of this technique in inhomogeneous and lossy background. The data used for the results presented here was "perfect" in the sense that there was no noise present in the system. The effect of the presence of noise on the reconstructions needs to be investigated. Because of the unavailability of the analytic expressions for scattering by complex geometry, the image quality for complicated objects has not been investigated yet.

It is proposed that numerical techniques, such as the Finite-Difference Time-Domain (FDTD) method, be used in conjunction with the software developed for this technique to make a larger class of objects accessible for investigation using this technique. This constitutes another area in which substantial work needs to be done. The extension of this technique to a larger class of objects, including strong scatterers, needs to be investigated. In this context, the combination of iterative techniques with the weak scattering approximation is an area that needs further research. An example of such an approach would be to use the iterative Born approximation [8] instead of a simple first-order Born approximation.

Before implementing this technique in the field, it is proposed that the measured values of the permittivity of coal-tar be first used in the simulations. This would provide a more accurate idea about the performance of this technique in actual implementation.

## 8. References

- [1] Mueller, R.K., Kaveh, M., and Wade, G., "Reconstructive Tomography and Application to Ultrasonics," Proc. IEEE, vol. 67, no.4, pp. 567-587, 1979.
- [2] Chu, T., and Lee, K., "Wide Band Microwave Diffraction Tomography Under Born Approximation," IEEE Trans. Antennas Prop., vol. 37, no. 4, pp. 515-519, 1989.
- [3] Devaney, A.J., "Geophysical Diffraction Tomography," IEEE Trans. Geosc. Remote Sensing, vol. GE-22, no.1, pp. 3-13, 1984.
- [4] Devaney, A.J., "Geophysical Diffraction Tomography in a Layered Background," Wave Motion, vol. 14, pp. 243-265, 1991.
- [5] Pan, S.X., and Kak, A.C., "A Computational Study of Reconstruction Algorithms for Diffraction Tomography: Interpolation Versus Filtered Backpropagation," IEEE Trans. Acoust., Speech, Signal Processing, vol. ASSP-31, no.5, pp. 1262-1275, 1983.
- [6] Stark, H., Woods, J.W., Paul, I., and Hingorani, R., "Direct Fourier Reconstruction in Computer Tomography," IEEE Trans. Acoust., Speech, Signal Processing, vol. ASSP-29, no.2, pp.237-245, 1981.
- [7] Witten, A.J., and Long, E., "Shallow Applications of Geophysical Diffraction Tomography," IEEE Trans. Geosc. Remote Sensing, vol. GE-24, no.5, pp. 654-662, 1986.
- [8] Chew, W.C., "Waves and Fields in Inhomogeneous Media," New York, Van Nostrand Reinhold, 1990.